Reviews in Aquatic Sciences, 6(2):121–137 (1992)

Phytoplankton Blooms at Fronts: Patterns, Scales, and Physical Forcing Mechanisms

Peter J. S. Franks

College of Oceanography, Oregon State University, Oceanography Administration Bldg. 104, Corvallis, OR 97331-5503

ABSTRACT: Numerous studies have shown phytoplankton blooms to be closely related to fronts in the ocean. The spatial and temporal patterns of the phytoplankton population depend on the predominant mode of physical forcing, and its scales of variability. Four types of fronts are examined here: wind-driven upwelling, water mass/buoyancy, tidal, and topographic. The phytoplankton pattern commonly found at each type of front is described. Finally, the scales of phytoplankton patchiness and the front itself are compared. It is found that there was no correlation between the scale of the front and the scale of its associated phytoplankton patch. This implies either that processes are acting to decorrelate the two fields, or that the forces mediating the enhanced production are not correlated with the length scale of the front. These possibilities are explored in detail.

KEY WORDS: phytoplankton patch, wind-driven upwelling, tidal front, buoyancy front, topographic front.

I. INTRODUCTION

Of the variety of forms of primary production in the ocean, perhaps the most spectacular is the formation of red tides. These massive blooms of single phytoplankton species have been seen the world over for centuries. Only now are we beginning to understand the mechanisms that cause and maintain red tides, and one property that appears to be common to most, if not all, red tides is their association with water mass discontinuities such as pycnoclines or fronts.

That fronts are typically the site of enhanced phytoplankton biomass suggests there may be processes common to various types of fronts that support such blooms. The present paper is an introductory review of the associations of phytoplankton blooms with fronts. First, the qualitative features of the phytoplankton patches at several types of fronts are described. Next, some physical mechanisms thought to cause the enhanced production are explored. This exploration is done by comparing the length scales of phytoplankton patches to the length scales of their fronts. From the results of this comparison, inferences are made concerning the types of physical processes most important to the phytoplankton at fronts. Before examining particular fronts in detail, however, the concepts of fronts and length scales are introduced.

A. Fronts

Fronts are regions of strong horizontal temperature and/or salinity contrast. They may occur in the atmosphere, lakes, rivers, and oceans. Here, we consider only a limited set of coastal oceanic fronts: wind-driven upwelling fronts, water mass or buoyancy fronts, tidally generated fronts, and topographically formed fronts.

Figure 1 shows a typical density pattern for a front. The upward bending of the pycnocline separating the lighter surface water from the dense deep water creates the front. The front need not always break through to the surface; subsurface fronts are also frequently seen. The pycnocline may also bow downward to intersect the bottom, creating a bottom front (Mooers et al., 1978). In the present paper, the width of the "frontal region" refers to the zone in which the pycnocline slopes upward or downward from the horizontal;

0891-4117/92/$.50

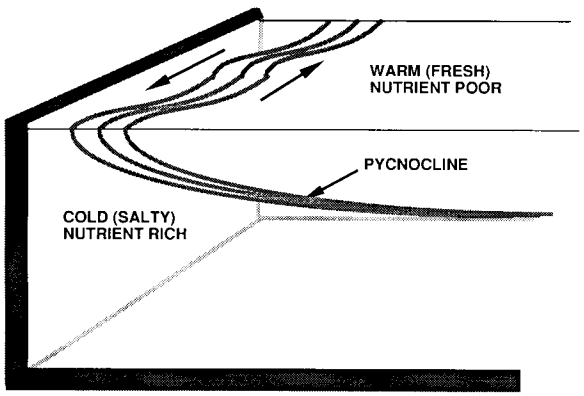

FIGURE 1. Typical density distribution at a front. The curved pycnocline forms the front and is the region of strongest along-front shear.

the width of the front refers to the horizontal extent of the density contrast at the surface or bottom. Thus, the frontal region will normally be wider than the front itself.

The balance of forces across the front (a strong pressure gradient vs. the Coriolis force) creates along-front jets, with the front being the zone of strongest shear. This jet can become unstable, forming cusps and eddies in the front (Pingree et al., 1974; James, 1988). The strength of the along-front jets and the general characteristics of the front depend on the mechanisms that cause and maintain the front. Thus, fronts formed by a surface wind stress will have a different character from ones formed by tidally induced bottom friction. However, certain generalities can be made about fronts, which can lead to insights into the mechanisms causing enhanced phytoplankton production there.

B. The Rossby Radius

The present paper examines the relationship of phytoplankton patches with a variety of different types of fronts. In order to make generalizations about these relationships, it would be useful to have a common basis with which to compare the different physical systems. The internal Rossby radius of deformation provides such a basis, giving the theoretical width scale of many kinds of frontal regions in the ocean.

When a front is formed, the pycnocline separating the two water masses becomes sloped, leading to a strong horizontal density contrast. The lighter water will always tend to flow over the more dense water to return the pycnocline to the horizontal. On a rotating Earth, however, this tendency to flow becomes balanced by the Coriolis force, which causes the flow to turn to its right in the northern hemisphere. Thus, rather than relaxing to the horizontal, the pycnocline remains sloped. The curvature of this slope (and thus the width of the frontal region) depends on the density contrast of the two water masses, their thicknesses, and the strength of the Coriolis force (i.e., latitude). This length scale is given by the Rossby radius of deformation and is shown in Figure 2.

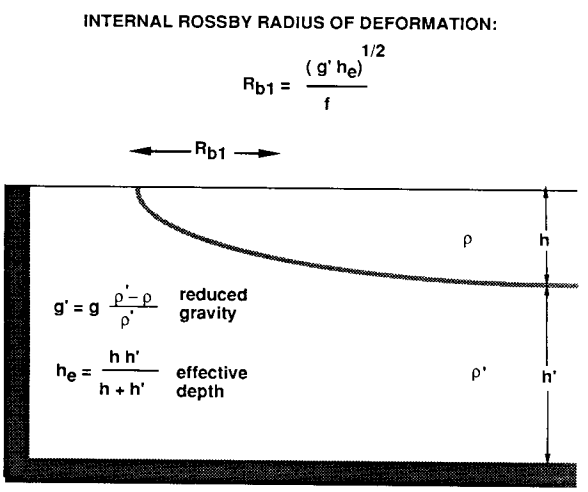

FIGURE 2. Calculation of the internal Rossby radius of deformation.

If we consider two water masses of densities ρ and ρ', and thicknesses h and h', we can define two parameters: the "reduced gravity" and the "effective depth." With g being the gravitational acceleration, the reduced gravity, g' (units of m s^{-2}), is given by:

$$g' = \frac{g(\rho' - \rho)}{\rho'} \qquad (1)$$

This is the buoyancy of one water mass relative to the other. The effective depth, h_e, is defined as:

$$h_e = \frac{hh'}{h + h'} \qquad (2)$$

With the reduced gravity, this equation allows the pycnocline in a two-layered system to be viewed as the free surface of a one-layered system, characterized by the effective depth h_e. The baroclinic Rossby radius of deformation, R_{b1}, is a combination of these parameters:

$$R_{b1} = \frac{\sqrt{g'h_e}}{f} \qquad (3)$$

where f is the Coriolis frequency. This formulation of the Rossby radius is applicable to fronts that have a pycnocline that becomes horizontal at some distance from the front. However, some fronts extend from the surface to the bottom, in which case another baroclinic Rossby radius of deformation, R_{b2}, is the appropriate length scale:

$$R_{b2} = \frac{\sqrt{g'(h + h')}}{f} \qquad (4)$$

Notice that this formulation uses the total depth of the water column rather than the effective depth. The R_{b2} scale is often applicable to water mass fronts, particularly river plume fronts, as is described later.

In many cases, the lower layer depth, h', is large relative to the surface layer thickness, h, so that $h_e \sim h$. In this instance, it is convenient to calculate the Rossby radius from

$$R_b = \frac{\sqrt{g'h}}{f} \qquad (5)$$

The Rossby radius scaling of the width of the frontal region is a useful theoretical tool for understanding the balance of forces at fronts. The Rossby radius of deformation gives the natural scale of pycnocline bending in the ocean. However, the assumptions inherent in its formulation, such as a sharp pycnocline, may render its application invalid. In more practical terms, it is often difficult to apply a calculated Rossby radius due to topography, external forces, or mixing. Thus, we must use some caution in applying a theoretically calculated Rossby radius to a field situation.

II. QUALITATIVE ASPECTS

In this section, four common types of fronts are described: wind-driven upwelling fronts, water mass or buoyancy fronts, tidally generated fronts, and topographically formed fronts. The mechanisms of formation of each front are outlined, and the typical Rossby radius given. Finally, the patterns of phytoplankton production that are commonly seen at these fronts are described.

A. Wind-Driven Coastal Upwelling

Fronts created by alongshore winds are common features along much of the world's most productive coastlines. These upwelling fronts have been intensively studied off the west coast of the U.S. (Mooers et al., 1976; Halpern, 1976), the northwest coast of Africa (Barton et al., 1977), and the south coast of Africa (Shannon, 1985). A persistent upwelling system off the coast of Peru did not show an associated front (Brink et al., 1983). Areas of persistent wind-driven coastal upwelling are some of the most productive oceanic zones; in particular, the upwelling region off Peru supported one of the most productive anchovy fisheries in the world (Rojas de Mendiola, 1981).

Wind-driven coastal upwelling (Figure 3) is generated by an alongshore windstress at the water's surface. For a north-south oriented coastline on the east side of an ocean basin, an equatorward windstress will generate upwelling, while a poleward windstress generates downwelling. An upwelling-favorable windstress creates an offshore Ekman flux within the surface layer. This offshore flux must be balanced by an onshore flow of deeper water, which causes the pycnocline to bend upward near the coast. For particularly strong or persistent winds, the pycnocline may intersect the surface and move offshore, creating a strong surface thermal front (Csanady, 1982).

The hydrographic signature of a wind-driven upwelling front is usually seen most strongly in the temperature field. A relatively well-mixed region inshore is composed of cold, nutrient-rich waters of deep origin. A narrow region of strong horizontal thermal gradient (the front) separates

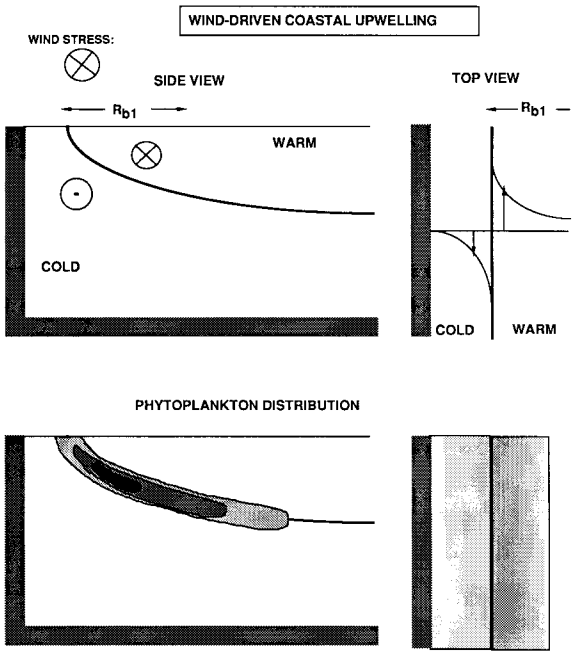

FIGURE 3. Upper panels show the hydrographic distributions at a wind-driven upwelling front. The lower panels indicate the distribution of chlorophyll commonly found at these fronts.

the cold, well-mixed inshore waters from the thermally stratified offshore region (Brink, 1983, 1985). The salinity contrasts across the front are generally small, with temperatures contributing the major part of the density difference.

The pycnocline that forms the front curves downward and offshore until it becomes horizontal. The length scale that governs this curvature is the baroclinic Rossby radius of deformation, R_b or R_{b1}. Typically, the value of R_{b1} is on the order of 10 km; however, in regions of steep bathymetry, the R_b scaling will be only approximately valid. It is also important to note that R_{b1} gives the scale of the curvature of the pycnocline, not the distance of the front from the shore (Brink, 1987).

A prominent chlorophyll maximum layer (measured as chlorophyll m^{-3}) is usually found just offshore of the front, within or slightly above the pycnocline (Jones and Halpern, 1981; Dengler, 1985; Traganza et al., 1987). The chlorophyll concentrations decrease rapidly toward the nearshore side of the front, and more gradually toward the offshore (stratified) side. The peak of the distribution generally follows the pycnocline as it curves downward, leading to a marked subsurface band of chlorophyll within the curved pycnocline. Satellite images of surface chlorophyll distributions show a strong surface signature in a banded structure oriented parallel to the isobaths (Abbott and Zion, 1985). This banding can extend for tens to hundreds of kilometers alongshore (Small and Menzies, 1981). Because of the curvature of the pycnocline, and the subsurface peak in chlorophyll, the surface signature does not generally reflect the subsurface distribution of chlorophyll. This can create difficulties when trying to interpret satellite images of pigment concentration.

The phytoplankton species making up the chlorophyll maximum layer vary depending on location and time of year. Diatoms of the genera *Thalassiosira, Nitzschia,* and *Chaetocerus* and dinoflagellates of the genera *Prorocentrum, Ceratium, Gyrodinium,* and *Gymnodinium* are commonly found in upwelling areas (Rojas de Mendiola, 1981; Blasco et al., 1981; Vincent et al., 1989). Dinoflagellates, in particular, have been found to reach red tide concentrations on occasion. A bloom of *Gymnodinium splendens* devastated the Peruvian fishery in 1976, reaching concentrations of 2000 cells per milliliter (Rojas de Mendiola, 1979).

B. Water Mass/Buoyancy Fronts

Water mass or buoyancy fronts (Figure 4) are created at the abutment of two dissimilar water masses. This may occur on a small scale at the mouth of an estuary (Garvine and Monk, 1974; Chao, 1987), or on a larger scale such as the Norwegian Current (Mork, 1981; Dundas et al., 1989) or the shelf-slope front off eastern North America (Houghton and Marra, 1983). These fronts often run parallel to a coast due to the nature of the formation of the inshore water mass, but this is certainly not always the case. In the Skagerrak/Kattegat areas, a strong water mass front was seen by Richardson (1985), the front being oriented perpendicular to the Danish coast.

The density contrast at a water mass front is caused by a salinity difference between the two water masses. The lighter water mass will tend to flow over the heavier water mass, until the pressure gradient is balanced by the Coriolis force, creating an approximately geostrophic balance

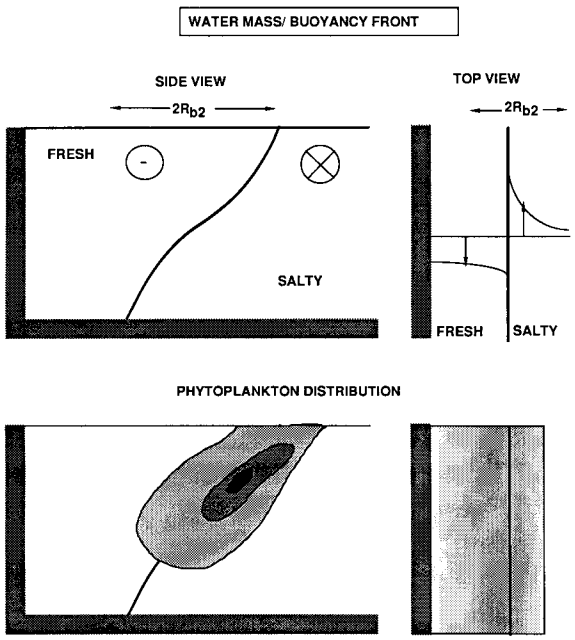

FIGURE 4. The hydrographic and dynamic signatures of water mass, or buoyancy fronts, are shown in the upper panels. The distribution of chlorophyll at these fronts is shown in the lower panels.

(Bowman and Iverson, 1978). Depending on the size and densities of the two water masses, and the bottom topography, the front may extend from the surface to the bottom, or from the surface to some equilibrium depth where the pycnocline becomes horizontal (Csanady, 1971). In either case, the pycnocline will slope downward from the surface, away from the more dense water mass. Thus, the front formed by estuarine outflow will always slope downward toward the coast, unless the plume has separated from the coast.

The water mass/buoyancy front will often have a curved/S-shape in a vertical cross section due to the flow of light water over the deeper heavy water. The width of the front is usually scaled by the baroclinic Rossby radius of deformation, R_{b2}. The horizontal distance from the surface of the front to the intersection of the front with the bottom is $2R_{b2}$. The width is usually a few kilometers, but may reach tens of kilometers in deep regions of high density contrast. The actual width of the frontal region is strongly influenced by the wind, which may increase it (flatten the front), or decrease it (steepen the front) (Csanady, 1971, 1978; Hsueh and Cushman-Roisin, 1983; Ou, 1984).

In general, the maximum chlorophyll value is found subsurface, within the front. The chlorophyll peak in vertical profiles is usually found in the pycnocline, giving a chlorophyll distribution that follows the isopycnals (Marra et al., 1982; Richardson, 1985). This is not always the case, though, since water mass fronts vary considerably in depth and horizontal extent of the pycnocline. In regions where the pycnocline becomes deeper than the euphotic zone, and depending on the source of the density contrast, the peak chlorophyll values may be found within the lighter (less saline) water, rather than the front itself (see, for example, Bowman and Iverson, 1979).

The distribution of dinoflagellates in water mass/buoyancy fronts is not always coincident with the chlorophyll distribution. Franks and Anderson (1992) found a bloom of *Alexandrium tamarense* within a buoyancy front, while the chlorophyll peak, created by a bloom of the diatom *Eucampia,* was offshore of the front. However, Blasco (1977) found a bloom of *Gonyaulax polyedra* that correlated well with the chlorophyll field in the California Current. In this case, the dinoflagellates composed up to 40% of the total phytoplankton numbers, whereas diatoms were only about 1%.

C. Tidal Fronts

Tidal fronts (Figure 5) are formed in shallow seas that have strong tidal currents and sloping bathymetry. Such areas are found around the British Isles (Pingree and Griffiths, 1978), the islands of Japan (Kishi and Ikeda, 1986), the northern areas of the Gulf of Maine (Yentsch and Garfield, 1981), and many other shallow seas. These fronts are often the site of intense dinoflagellate blooms.

The motion of water over the bottom generates turbulence, much the same way as windstress at the surface. Tidally forced motions of the water are ubiquitous, although the local strength of the tidal currents is a function of basin shape and topography. In shallow waters, a sufficiently strong tidal current can generate turbulence that can mix the overlying waters. In deeper waters, the same turbulence may not mix

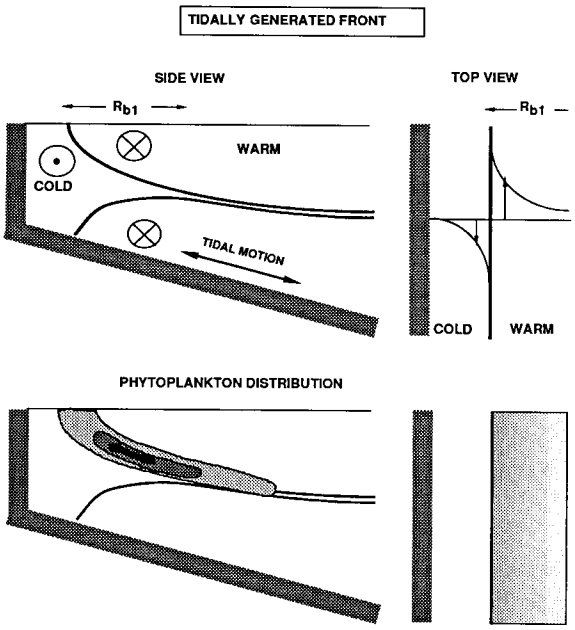

FIGURE 5. The hydrographic and dynamic signatures of tidally generated fronts are shown in the upper panels. The distribution of chlorophyll at these fronts is shown below.

high enough into the water column to affect the pycnocline. The region separating the well-mixed zone inshore from the stratified offshore waters is the tidal front.

The location of tidal fronts has been shown to be predictable through the H/u^3 criterion of Simpson and Hunter (1974). This criterion uses H, the depth of the water column, and u, the tidal velocity, to identify regions that should be either well mixed or stratified. A critical value of H/u^3 can often be found that will give the location of tidal fronts. This value varies geographically depending on local heat input and windstress (Garrett et al., 1978; Loder and Greenberg, 1986). Heating will tend to move tidal fronts inshore, as it will oppose the mixing from below, while windstress will move tidal fronts offshore by increasing the total turbulent kinetic energy.

The front created between the well-mixed inshore waters and the stratified offshore waters is usually seen most clearly in the temperature profiles. The mixing inshore creates an approximately isothermal water mass, giving a strong thermal contrast across the surface of a tidal front. The pycnocline generally surfaces, curving downward and offshore; however, the lower part of the pycnocline may intersect the bottom if the inshore water mass has the same density as the water forming the pycnocline. The formation of this bifurcated pycnocline is dependent on the initial densities and volumes of the two water masses (surface and deep) (van Heijst, 1986). The curvature of the pycnocline, i.e., the length scale of the front, is given by R_{b1}, the baroclinic Rossby radius of deformation. This length scale is usually <5 km, indicating a rather narrow frontal zone.

A marked chlorophyll maximum layer is often found within the pycnocline forming the tidal front (Holligan, 1981). The peak chlorophyll values are normally subsurface, slightly offshore of the front (i.e., on the stratified side) (Savidge, 1976; Pingree et al., 1978; Simpson et al., 1979; Holligan et al., 1983). The chlorophyll contours follow the pycnocline, decreasing as the pycnocline becomes more horizontal. The inshore waters, although often nutrient rich, generally have a low concentration of phytoplankton due, perhaps, to light limitation caused by enhanced vertical mixing. Tidal fronts are often the site of intense dinoflagellate blooms (see, for example, Pingree et al., 1975; Holligan, 1981). Local concentrations of *Gyrodinium aureolum* reached 1.7×10^6 cells/l in tidal fronts around the British Isles, giving integrated chlorophyll concentrations 40 times higher than the surrounding waters (Pingree et al., 1975). Simpson et al. (1979) found a tenfold increase of *Peridinium trochoideum* within a tidal front compared to surrounding waters.

The phytoplankton community structure within tidal fronts is often predictable: the inshore waters are dominated by diatoms, the surface waters on the stratified side usually contain mainly small flagellates, while the front and pycnocline are the sites of dinoflagellates and diatoms (Pingree et al., 1978). This follows Margalef's (1978) description of the ontogeny of phytoplankton communities in response to physical forcings (see also Legendre et al., 1986).

D. Topographic Fronts

Topographic fronts (Figure 6) are formed in the lee of stationary objects embedded in a flow.

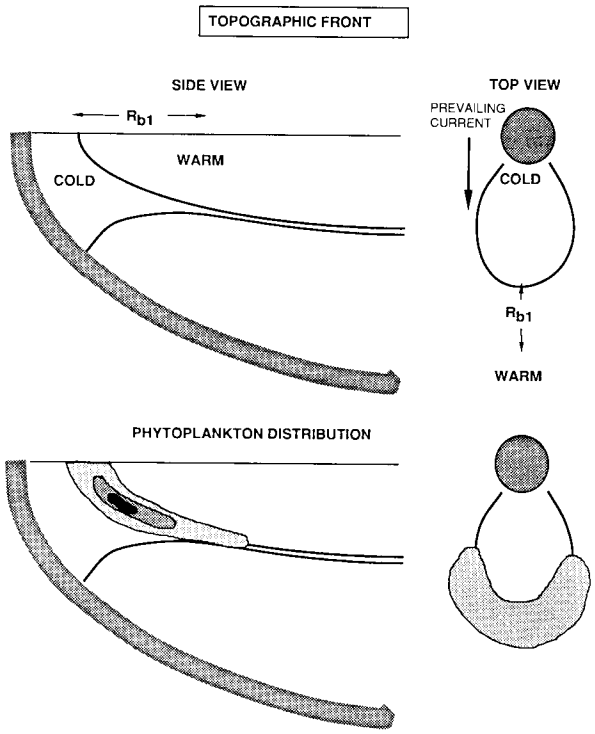

FIGURE 6. The hydrographic signature of topographically generated fronts is shown in the upper panels. The chlorophyll distribution commonly found at these fronts is shown below.

Thus, they are found near islands and headlands in areas of strong currents (Pingree and Griffiths, 1978; Pingree and Maddock, 1979). If the current is normally from one direction, the topographic front may be stationary relative to the object, giving a predictable hydrographic signature. In areas dominated by tidal flows, two topographic fronts are formed around the flanks of an island, perpendicular to the main axis of the tidal ellipse (Wolanski et al., 1984).

As a stratified fluid flows past a stationary object, mixing will take place in the lee of the object. As with the tidal front, this mixing generates a third water mass, with temperatures and salinities some average of the surface and deep water masses. The boundary between the well-mixed water in the lee of the topographic feature and the stratified water farther away is the topographic front.

The pycnocline of a topographic front slopes down from the surface and away from the topographic feature that generated the front. It can also bifurcate in the same manner as a tidal front, creating both surface and bottom fronts (Simpson et al., 1982; Wolanski et al., 1984). The length scale that governs the steepness (and thus the width) of the front is the baroclinic Rossby radius of deformation, R_{b1}. As with tidal fronts, this length is often <5 km.

The front is usually seen most strongly in the horizontal temperature contrast. Cold water near the topographic feature indicates the region of intense mixing, while the warmer, stratified waters further away reflect the influence of solar heating (Pingree and Griffiths, 1978). In plane view, the front tends to be curved, either surrounding the topographic feature, or forming a tear-drop shape intersecting the topographic feature at its narrow end (Simpson et al., 1982; Simpson and Tett, 1986). This is in contrast to the fronts described above, which tend to form long, relatively straight fronts extending for considerable distances (tens to hundreds of kilometers). In many cases, the front is formed by an eddy in the lee of the topographic feature. Wolanski et al. (1984) present a simple model for eddy formation and suggest some basic criteria for the size of the eddy and circumstances under which it will form. Unfortunately, calculation of these parameters requires measurement of values such as the vertical velocities and vertical eddy diffusion coefficient, both of which are extremely difficult to measure.

The distribution of chlorophyll within topographically formed fronts is similar to that of tidally generated fronts. A subsurface chlorophyll maximum is found just offshore of the front, while the chlorophyll maximum layer follows the sloping pycnocline. This puts the chlorophyll maximum on the side of the front away from the topographic feature (Pingree and Griffiths, 1978; Townsend et al., 1983). Although these fronts have not been shown to have the same distribution of phytoplankton classes as tidal fronts, the similarity of hydrography suggests that this may be the case. Indeed, high concentrations of the dinoflagellate *G. aureolum* were found within a topographic front near the British Isles (Simpson et al., 1982).

III. QUANTITATIVE ASPECTS

One obvious question that arises from the preceding discussion is, "If the frontal structure

is determined by Rb, then is the phytoplankton distribution at a front also scaled by the Rossby radius of deformation?'' To answer this, we must calculate the length scale of the chlorophyll maximum within the front and the appropriate Rossby radius for that front.

The length scale of the phytoplankton distribution was calculated using the method shown in Figure 7. First, the horizontal axis zero was set at the location of the phytoplankton maximum. The distance from this zero to each of the contours within the pycnocline (i.e., not necessarily at the same depth) was measured. With these data, the phytoplankton (chlorophyll, cell counts, etc.) could be plotted vs. x, the horizontal distance along the pycnocline. The model

$$\mathrm{Chl}(x) = \mathrm{Chl}_{\infty} + \mathrm{Chl}_{max} \exp(-x/L) \quad (6)$$

was then fit to the data. Here Chl_{max} is the chlorophyll (cell count) at x = 0, i.e., the chlorophyll maximum, and Chl(x) is the predicted chlorophyll (cell count) distribution. Chl_{∞} is the concentration of chlorophyll in the pycnocline far away from the front (Chl(x) as $x \rightarrow \infty$). The parameter L, which is given by the regression, is the length scale of the phytoplankton patch. It is important to note that this length scale does not give the width of the patch at a given depth, but rather the width of the patch along an isopycnal. In doing this, we calculate a patch length scale that can be compared to the physical length scale.

Normalizing the chlorophyll data by Chl_{max}, and the length scales by the calculated Rossby radius allows comparison of the data from a variety of fronts. This will give us two nondimensional numbers to plot: $(\mathrm{Chl}(x) - \mathrm{Chl}_{\infty})/(\mathrm{Chl}_{max} - \mathrm{Chl}_{\infty})$ vs. x/R_{bi}. If $L = R_{bi}$ (patch length = Rossby radius), all the points will lie along the line $y = \exp(-x)$. If $L > R_{bi}$ (patch length > Rossby radius), the points will lie above this line, and vice versa.

Eight data sets were utilized for this analysis, shown in Table 1. These data sets include a variety of fronts over a wide geographic range. The results are plotted in Figure 8, which show quite clearly that the phytoplankton patch length scales are not equal to the theoretical Rossby radius of deformation. However, it also indicates that the

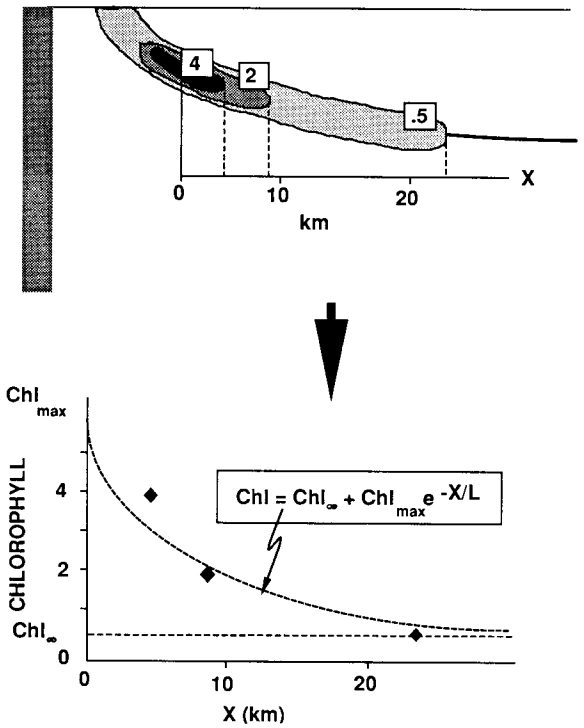

FIGURE 7. The method for calculating the phytoplankton patch length scale is illustrated here. The parameter L, given by the regression, is the patch length scale.

patch length is always greater than the Rossby radius, generally 5 to 10 times greater. Thus, rather than a phytoplankton patch being on the order of 5 km in cross-frontal width, the patches are normally 25 to 100 km in width.

Having shown that the phytoplankton patch length scale is not equal to the Rossby radius, it is appropriate to ask, ''Is the measured physical frontal length scale equal to the theoretically calculated Rossby radius?'' To answer this question, we take a similar approach to that above, but trace the depth, h(x), of an isopycnal from the front (h(0) = 0) to its equilibrium depth, h_0, the depth at which the pycnocline becomes horizontal. Plotting $h_0 - h(x)$ vs. the horizontal distance, x, will give a horizontal profile of the depth of the isopycnal. However, we can normalize the axes in the same manner as above by dividing $(h_0 - h(x))$ by h_0, and x by R_b. This nondimensionalization will allow us to plot all the fronts on one set of axes. If the calculated frontal length scale is equal to its Rossby radius, all the points will lie along the curve $y = \exp(-x)$. Fronts

TABLE 1
Data Sets Used in Analysis

Data set	Type of front	Frontal scale (km)	Rossby radius (km)
Simpson et al. (1982)	Topographic	6.25	4.3
Franks and Anderson (1991)	Buoyancy	1.2	6.5
Richardson et al. (1985)	Water mass	4.5	2.5
Richardson (1985)	Water mass	1.9	7.5
Holligan (1981)	Tidal	37.0	4.5
Tett (1981)	Tidal	3.4	1.5
Jones et al. (1986)	Upwelling	20.0	7.5
Small and Menzies (1981)	Upwelling	7.5	7.0

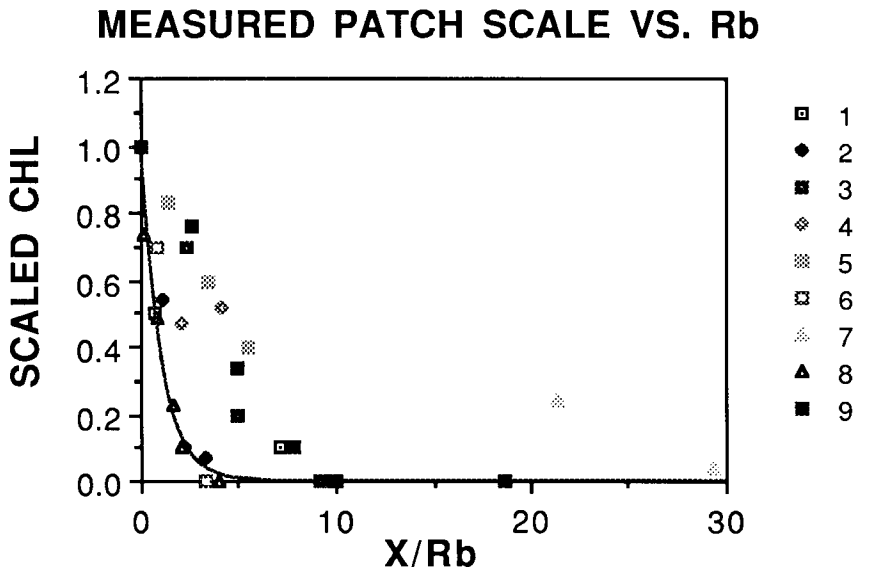

FIGURE 8. A plot of chlorophyll (cell count, etc.) vs. horizontal distance, x. The vertical axis has been scaled by Chl_{max}, the maximum chlorophyll (cell count, etc.) for a given data set, while the horizontal axis has been scaled by the Rossby radius. The solid line is $y = \exp(-x)$. The data sets indicated are (1) Simpson et al. (1982); (2) Franks and Anderson (1992); (3) Richardson et al. (1985); (4) Richardson (1985; April 6); (5) Richardson (1985; April 8); (6) Holligan (1981); (7) Tett (1981); (8) Jones et al. (1986); (9) Small and Menzies (1981).

with length scales longer than the Rossby radius will lie above this curve and vice versa.

Figure 9 shows that the frontal length scale is not equal to the theoretically calculated Rossby radius. In fact, it appears that the frontal scale is always larger than the Rossby radius, indicating that the front is more relaxed (less steep) than would be predicted on the basis of the Rossby radius alone. This is not too surprising, given the number of mechanisms that can relax the front. These include friction within the front, alongshore processes such as windstress or bottom friction, nonzero vorticity, instabilities along the front, and eddy formation across the front.

Since both the phytoplankton patch length scale and the frontal length scale are greater than the theoretical Rossby radius of deformation, perhaps they are equal to each other. Thus we ask, "Are the phytoplankton patch and frontal length scales equal?" In this case, we can plot the phytoplankton patch length scales vs. the frontal length scales calculated above. If they are equal, the points should lie along the 1:1 line on the plot. Such a plot is shown in Figure 10. From

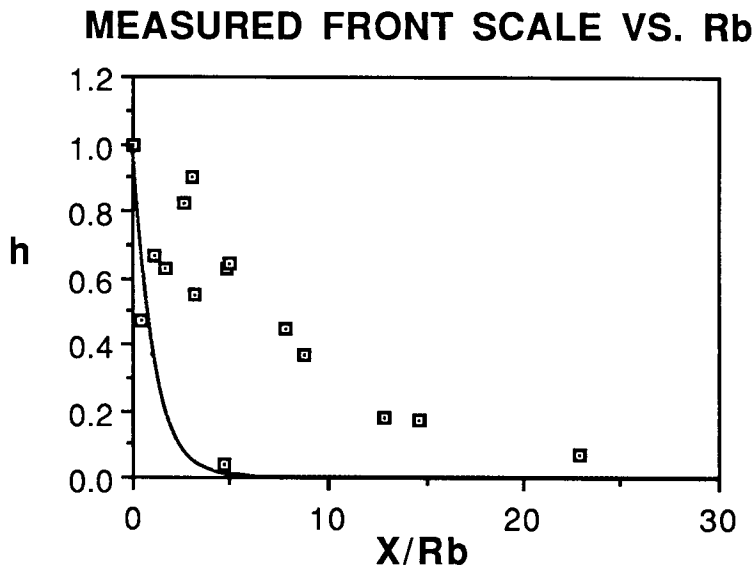

FIGURE 9. Here the scaled pycnocline depth is plotted vs. scaled horizontal distance. The pycnocline depth, h, has been scaled by the equilibrium pycnocline depth, h_0, and the horizontal distance scaled by the Rossby radius. The solid line is $y = \exp(-x)$.

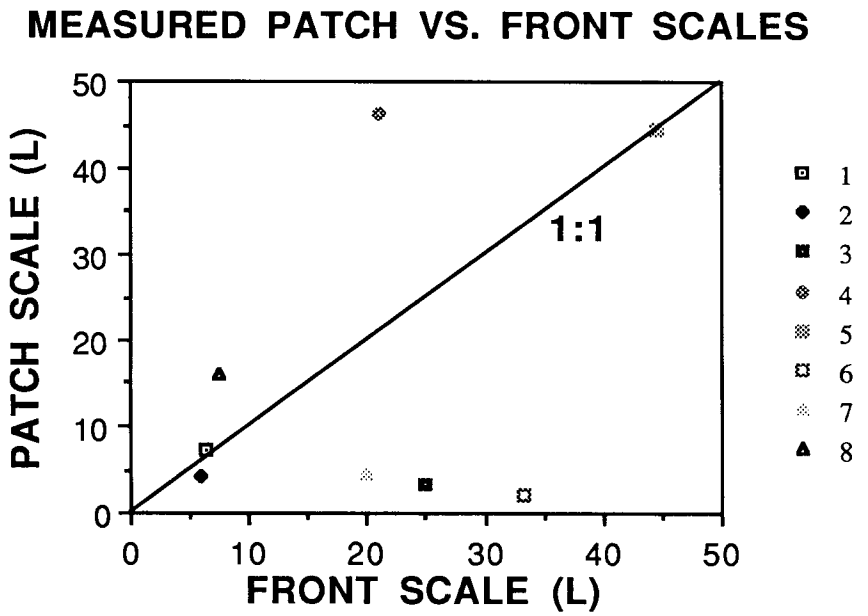

FIGURE 10. Here the measured phytoplankton patch scale is plotted against the measured frontal scale. The solid line represents a 1:1 relationship. The data sets indicated are (1) Simpson et al. (1982); (2) Franks and Anderson (1992); (3) Richardson et al. (1985); (4) Richardson (1985); (5) Holligan (1981); (6) Tett (1981); (7) Jones et al. (1986); (8) Small and Menzies (1981).

this plot, it is obvious that there is no relation between the patch size and the frontal scale, i.e., the points are scattered and do not lie near the 1:1 line.

The lack of a correlation between the patch size and frontal scale suggests two possibilities: (1) the length scales should be correlated; (2) the length scales should not be correlated.

If we assume (1), we seek mechanisms that would decorrelate the patch and frontal length scales. If we assume (2), we must look for processes that would enhance phytoplankton growth at a front, but that do not have a length scale dependent on the front. By exploring each of the two possibilities, we should gain insight into the mechanisms driving the enhanced phytoplankton production at fronts.

A number of processes exist that would decorrelate phytoplankton patch and frontal length scales. The most obvious of these is a mismatch of the timescales of frontal development and phytoplankton growth. Walsh et al. (1977) suggest that the "event" timescale for wind-driven upwelling is about 3 days. This includes spin-up, frontal formation, and spin-down. With a growth rate of 1 day^{-1}, the phytoplankton would take at least 1 day, and probably closer to 5 days, to show a significant response to such an event. Thus, the front could have formed and relaxed before the phytoplankton population could "catch up". This has been demonstrated by Jones and Halpern (1981), who found the primary productivity to peak about 5 days after the maximum in nitrate, and about 10 days after the onset of upwelling. Dugdale and Wilkerson (1989) give evidence to support the model of Wilkerson and Dugdale (1987), suggesting that the timescale to complete nutrient depletion following an upwelling event is about 10 days. Small and Menzies (1981) examined historical data from the western coast of the U.S., looking for situations in which the wind-driven upwelling should have reached and maintained a steady state over several days. Their data show that the frontal and patch length scales are equal under these conditions. This suggests that a mismatch of timescales could be an important decorrelation mechanism for wind-driven upwelling.

A further effect of a mismatch of environmental and physiological timescales is the spreading and attenuation of a biomass peak as it propagates through various trophic levels (Denman et al., 1989). A pulse of nutrient forced into the euphotic zone by a physical process (e.g., wind-driven upwelling) will be converted to phytoplanktonic biomass over a period of days, and into crustacean biomass over weeks. During this time, the original biomass peak spreads throughout the community and is translocated by the prevailing currents. Thus, the community response to physical events is complex, dependent on time, space, and size class, and may result in a strong decorrelation of biomass signatures from the physical forcing.

Tidal fronts show predominantly semidiurnal, diurnal, and fortnightly variations, driven by the M_2 and K_1 tides. The M_2 tide not only creates and maintains the tidal front, but it also advects it back and forth along the long axis of the tidal ellipse. Superimposed on this semidiurnal variation is the fortnightly spring-neap cycle. The variation in tidal velocity associated with these two components will alter the strength of the front, and the light, temperature, and nutrient regime of the phytoplankton (Demers et al., 1986). The fortnightly variation is slow enough that the phytoplankton may respond to this forcing (Balch, 1981), but the diel variation may keep the phytoplankton from reaching a steady state within the front. On the other hand, the predictable regularity of the tides may create a niche that certain phytoplankton species can exploit, aiding the formation of the high production seen at tidal fronts (Margalef, 1978; Legendre et al., 1986).

The formation of topographic fronts may be dependent on tidal flows, or seasonal flows such as the gyre in the Gulf of Maine. Similarly, water mass or buoyancy fronts are often strongly seasonally variable, but show relatively small variations over days. Since the timescale of variation of these fronts is long relative to the generation time of phytoplankton, we would expect the phytoplankton to correlate well with the physical system.

Thus, it would appear that, except for wind-forced flows and the semidiurnal tide, the phytoplankton at most fronts should be able to track the variations in the physical system, and so should be closely correlated with the front. It seems, then, that mismatch of timescales of variation is not a sufficient explanation for the lack of a relationship between phytoplankton patch scales and frontal scales.

If we make the assumption that the patch and frontal length scales should not, *a priori*, be correlated, we must look for physical forcings that could enhance phytoplankton production at fronts,

but that have a length scale independent of the front. One such process is diffusion.

Diffusion acts to smooth gradients of a property, by mixing adjacent parcels. As such, it has no inherent length scale, although the magnitude of the mixing may depend on the distance over which the mixing takes place (Okubo, 1971). Fronts are very dynamic regions and have been predicted to have correspondingly strong mixing (see, for example, Mooers et al., 1978). This would imply that the magnitude of the diffusion coefficient is linked to the front (i.e., the slope of the pycnocline). The few measurements that have been made to test this, however, do not indicate any systematic enhancement of mixing within or around the front (The Coastal Transition Zone Group, 1988). This suggests that the diffusion scales should be independent of the frontal scales.

There are three main ways by which diffusion can affect the phytoplankton distributions. The first is by altering phytoplankton residence time in the water column. Pingree et al. (1975) calculated timescales for diffusion within a tidal front and suggested that phytoplankton in the well-mixed waters below the thermocline should be quickly dispersed, negating any accumulation of chlorophyll in this area. Similar arguments may apply to the surface mixed layer, although the vagaries of the wind make this a difficult calculation. Within the thermocline, however, the stratification reduces the mixing, giving a phytoplankton residence time that is long compared to their growth rate.

Vertical mixing will also affect the photoadaptation of the cells (Marra, 1978; Lewis et al., 1984) by mixing the cells through a light gradient. This may adversely affect certain species of phytoplankton that cannot respond to high-frequency light fluctuations (Harris, 1980). In addition, vertical mixing may cause light limitation if the mixing layer is deeper than the euphotic zone (Sverdrup, 1953). Thus, phytoplankton growth may be reduced in regions of enhanced vertical mixing, such as the unstratified waters near a front, or the surface waters on the stratified side of a front. This reduced growth may enhance the vertical and horizontal contrast of phytoplankton biomass in the various water masses. However, such processes will not explain the enhanced biomass generally seen at fronts.

The second influence of diffusion takes place through mixing of nutrients. Most fronts form a boundary separating a pool of dense, well-mixed, nutrient-rich water from more stratified nutrient-poor waters. Mixing of the two water masses will bring some of the nutrient-rich water into the euphotic zone on the stratified side of the front. This can be a significant source of nutrients for phytoplankton production at fronts (Loder and Platt, 1985). Dewey and Moum (1990) note that the wind-driven turbulence in the surface mixed layer can cause increased entrainment in regions where the pycnocline is shallow. This could result in enhanced nutrient supplies to phytoplankton growing on the stratified side of a front.

Tett (1981) and Traganza et al. (1987) used one-dimensional (vertical) models to try to evaluate the contribution of various processes to the phytoplankton at tidal and wind-driven fronts, respectively. In both cases, vertical diffusion and entrainment was found to account for the bulk of the production. Smith et al. (1983) employed a two-dimensional (cross-front) model that suggested that vertical diffusion was more important than cross-frontal advection in supplying phytoplankton and nutrients to the frontal zone.

The third mode of influence of diffusion on phytoplankton is through the physical act of mixing. It is well known that dinoflagellates are very sensitive to mixing. They are normally found in stratified waters in the field and do not tolerate mixing in laboratory cultures (see, for example, White, 1976). The reasons for this are not well understood. Based on evidence from the field, however, it is possible to predict the conditions that favor dinoflagellate growth (see, for example, Margalef, 1978; Legendre et al., 1986). In general, dinoflagellates are not found in well-mixed water columns, such as those seen on the nonstratified side of fronts. However, this does not present a mechanism by which phytoplankton production could be enhanced at fronts. Rather, it gives a mechanism whereby certain species may be reduced in regions surrounding the front.

The modes of diffusion most likely to enhance phytoplankton production at fronts are the effects on the phytoplankter's light environment and the transport of nutrients. This is the same conclusion arrived at by Yentsch (1974) and Loder and Platt (1985), although through quite different reasoning. The effects of these processes will be

expressed at, and near, the front. Here the mixed layer becomes very shallow, and the nutrient-rich water is near the surface, in close proximity to the stratified waters. This may explain the association of the phytoplankton maximum with the pycnocline, on the stratified side of the front. Such arguments suggest that the enhanced phytoplankton production should be similarly restricted. As can be seen from Figure 10, however, this is not necessarily the case. It is possible that some mechanism, such as cross-frontal circulation, is acting to spread the cells along the pycnocline, away from the front.

Cross-frontal circulations are thought to be vertical circulation cells with either one closed loop (see, for example, Csanady, 1975; Allen, 1980; Tang, 1983), or more commonly, two-closed loops such as described by Simpson et al. (1978) and Garrett and Loder (1981) for tidal fronts, or Foo (1981) and de Szoeke and Richman (1984) for wind-driven fronts. Such two-celled circulation patterns usually show a convergence zone at the front, with downwelling along the pycnocline. The upwelling from the deep water mass, followed by convergence at the front and downwelling within the pycnocline, may supply the phytoplankton within the pycnocline with nutrients otherwise unavailable to them. Although the cross-frontal flows should have the same length scales as the front itself, the advection within the pycnocline could act to decorrelate the phytoplankton populations from the frontal scales. This is supported by the model of Wilkerson and Dugdale (1987), which describes the "conveyor-belt" hypothesis for phytoplankton production in a wind-driven upwelling zone. Thus, the peak in production should be physically removed from the main upwelling region due to cross-frontal advection coupled with the delayed response of phytoplankton to new nutrients ("shift-up"). This hypothesis appears to be supported by the extensive observations of Dugdale and Wilkerson (1989) in the Point Conception region of California. Garrett and Loder (1981) used scaling arguments to suggest that frictionally induced cross-frontal flows within tidal fronts may be the predominant mode of cross-frontal transfer of properties at these types of fronts. Loder and Platt (1985), however, calculate that only about 6% of the nitrate flux to the phytoplankton on Georges Bank was due to cross-frontal circulations.

A secondary effect of the cross-frontal circulation is the possibility of enhanced vertical mixing due to shear within the frontal zone. Halpern (1976) showed the shear to increase, and the stratification to decrease, during a wind event, suggesting vertical mixing within the pycnocline. Winant (1980) found a similar situation and noted that the zone of maximal shear was found just below the thermocline. This observation may explain the measurements of Pingree et al. (1978), who found that the chlorophyll maximum layer was in the deeper portion of the pycnocline, but above the nitracline. Thus, a vertical supply of nitrate to these cells could take place by mixing only across the nitracline rather than the pycnocline. Such mixing should lead to a higher local chlorophyll concentration and may increase the vertically integrated chlorophyll, depending on the rate of supply of new nutrients below the pycnocline.

The models of Foo (1981) and de Szoeke and Richman (1984) both indicate that localized regions of enhanced turbulence form within the frontal zone. In the model of Foo (*op. cit.*) in particular, the nonuniform vertical diffusion of density acts to generate upwelling from below the pycnocline. A further effect of this vertical mixing is to locally vary the effective Rossby radius of deformation. Thus, such shear-induced mixing may influence the phytoplankton production through the vertical advection of phytoplankton and nutrient-rich water, while decorrelating the physical and biological scales.

IV. DISCUSSION

The strong association of enhanced phytoplankton biomass with fronts has been described for a variety of cases. Qualitatively, the chlorophyll maximum is usually associated with the pycnocline forming the front and is found subsurface on the stratified side of the front. Quantitatively, the scale of the phytoplankton patch was not found to be related to the theoretical scale of the front, or the actual scale of the front. The implications of this were discussed in terms of the processes mediating phytoplankton dynamics at fronts.

From the arguments thus presented, it appears that the enhanced phytoplankton produc-

tion at fronts is uncorrelated with the scale of the front itself. This implies that either there are processes decorrelating the patch and front scales, or the processes generating the phytoplankton patch are uncorrelated with the scale of the front. There appears to be more evidence from the literature to support the latter conclusion, except in very variable systems such as wind-driven upwelling. It is suggested that diffusive mixing is a major contributor to the phytoplankton production at fronts.

The effects of diffusion should be manifested in both the biomass of phytoplankton and their growth rates. Thus, the front should be the location of enhanced phytoplankton productivity, as well as production. This inference is supported by a variety of studies at fronts. Traganza et al. (1987) and Dengler (1985) both found the highest productivity just offshore of a wind-driven upwelling front. Jones and Halpern (1981) corroborate this finding and note that enhancement of productivity may show a lag of several days from the formation of the front. Holligan et al. (1984) and Videau (1987) showed primary productivity to peak within a tidal front off Ushant. However, when normalized to the amount of pigment present, Holligan et al. (*op. cit.*) showed the phytoplankton in the front to have a lower specific production rate than those in the surrounding waters. This finding is contradicted by that of Videau (*op. cit.*), who found the highest specific production rates to occur within the front. Richardson (1985) found an enhancement of primary production at a water mass front in the North Sea, giving daily production rates up to 25 times those of surrounding waters.

There are certain limitations to the methods used above that deserve some mention. From a theoretical point of view, the calculation of a Rossby radius is often problematic. The actual bottom topography may render the calculated radius invalid, or require the use of a spatially varying radius of deformation. Thus, our rather simple-minded approach to the application of the Rossby radius may not always apply.

As was previously mentioned, many physical processes will alter the structure of a front, so that the Rossby radius no longer scales the width of the front. These processes include internal friction, which will tend to relax (flatten out) a front; wind stresses, which can steepen or flatten a front; heat exchange, which can alter the buoyancy distribution; and a host of other processes operating on a variety of temporal and spatial scales.

From a more practical point of view, the data used to estimate patch and frontal scales may be insufficient for the purpose. If the theoretical Rossby radius is only a few kilometers, then the station spacing should be of the same order or less for the calculation of scales. In most cases, however, the station spacing is considerably larger. This means that the front may be much steeper than indicated in the data, and the scale that we are measuring is not the internal Rossby radius of deformation. A comparison of the fronts shown in Brink (1983, p. 235) to those of Halpern (1976) clearly demonstrate the difference station spacing makes in interpreting frontal scales. The pycnocline in Brink (*op. cit.*) is extremely steep near the surface, implying a short Rossby radius. The wider station spacing in Halpern (*op. cit.*) suggests a much more relaxed pycnocline, with a length scale on the order of 20 km. In fact, the pycnocline may have been as steep as in Brink (*op. cit.*), but the widely spaced stations obscure this.

The same caveats apply to the calculations of the phytoplankton patch scales. Phytoplankton concentrations are known to fluctuate over a range of scales (Platt, 1972); the scales measured here include just one band of the frequency range of patchiness. Thus, we would expect some variance about the values chosen as representative of a particular point in time and space. It is assumed, however, that this variance is relatively constant about a spatially varying mean; it is the shape of this mean which defines the phytoplankton "patch".

With these limitations in mind, it is clear that the methods reviewed still provide us with some clues to the processes mediating enhanced phytoplankton production at fronts. To better understand the processes hypothesized to be important, we must continue to make measurements on a variety of scales within frontal systems. In doing so, we may eventually learn how processes occurring on small scales can affect production over much larger scales, and gain a better understanding of the dynamics of red tides.

ACKNOWLEDGMENTS

I am pleased to acknowledge the helpful comments of D. Anderson, K. Brink, J. Cullen, J. Marra, and two anonymous reviewers. This work was supported by Office of Naval Research contract N00014-87-0007 and grants N00014-89-J-111 and N00014-90-J-1051.

REFERENCES

Abbott, M. and P. Zion. 1985. Satellite observations of phytoplankton variability during an upwelling event. *Cont. Shelf. Res.* **4**:661–680.

Allen, J. S. 1980. Models of wind-driven currents on the continental shelf. *Annu. Rev. Fluid Mech.* **12**:389–433.

Balch, W. M. 1981. An apparent lunar tidal cycle of phytoplankton blooming and community succession in the Gulf of Maine. *J. Exp. Mar. Biol. Ecol.* **55**:65–77.

Barton, E. D., A. Huyer, and R. L. Smith. 1977. Temporal variation observed in the hydrographic regime near Cabo Corveiro in the northwest African upwelling region, February to April 1974. *Deep-Sea Res.* **24**:7–23.

Blasco, D. 1977. Red tide in the upwelling region of Baja California. *Limnol. Oceanogr.* **22**:255–263.

Blasco, D., M. Estrada, and B. H. Jones. 1981. Short-time variability of phytoplankton populations in upwelling regions — the example of northwest Africa. **In:** *Coastal Upwelling*, pp. 339–347. (F. A. Richards, Ed.) Washington, D.C.: American Geophysical Union.

Bowman, M. J. and R. L. Iverson. 1978. Estuarine and plume fronts. **In:** *Oceanic Fronts in Coastal Processes*, pp. 87–104. (M. Bowman and W. Esaias, Eds.) New York: Springer-Verlag.

Brink, K. H. 1983. The near-surface dynamics of coastal upwelling. *Prog. Oceanogr.* **12**:223–257.

Brink, K. H. 1985. Some aspects of the physical processes in coastal upwelling. *Int. Symp. Upw. W. Afr., Inst. Inv. Pesq., Barcelona.* **1**:5–14.

Brink, K. H. 1987. Upwelling fronts: implications and unknowns. **In:** *The Benguela and Comparable Ecosystems.* (A. I. L. Payne, J. A. Gulland, and K. H. Brink, Eds.) *S. Afr. J. Mar. Sci.*, 5:3–9.

Brink, K. H., H. Halpern, A. D. Huyer, and R. L. Smith. 1983. The physical environment of the Peruvian upwelling system. *Prog. Oceanogr.* **12**:223–257.

Chao, S.-Y. 1987. Wind-driven motion near inner shelf fronts. *J. Geophys. Res.* **92**:3849–3860.

Csanady, G. T. 1971. On the equilibrium shape of the thermocline in a shore zone. *J. Phys. Oceanogr.* **1**:263–270.

Csanady, G. T. 1978. Wind effects on surface to bottom fronts. *J. Geophys. Res.* **83**:4633–4640.

Csanady, G. T. 1982. *Circulation in the Coastal Ocean.* Boston: Reidel Publishing Co., 280 p.

Demers, S., L. Legendre, and J.-C. Therriault. 1986. Phytoplankton responses to vertical tidal mixing. **In:** *Lecture Notes on Coastal and Estuarine Studies 17: Tidal Mixing and Plankton Dynamics*, pp. 1–40. (M. J. Bowman, C. M. Yentsch, and W. T. Peterson, Eds.) Berlin: Springer-Verlag.

Dengler, A. T. 1985. Relationship between physical and biological processes at an upwelling front off Peru, 15°S. *Deep-Sea Res.* **32**:1301–1315.

Denman, K. L., H. J. Freeland, and D. L. Makas. 1989. Comparisons of time scales for biomass transfer up the marine food web and coastal transport processes. **In:** *Effects of Ocean Variability on Recruitment and an Evaluation of Parameters Used in Stock Assessment Models*, pp. 255–264. (R. J. Beamish and G. A. McFarlane, Eds.) *Can. Spec. Publ. Fish. Aquat. Sci.*, 108.

De Szoeke, R. A. and J. G. Richman. 1984. On wind-driven mixed layers with strong horizontal gradients — a theory with application to coastal upwelling. *J. Phys. Oceanogr.* **14**:364–377.

Dewey, R. K. and J. N. Moum. 1990. Enhancement of fronts by vertical mixing. *J. Geophys. Res.* **95**:9433–9445.

Dugdale, R. C. and F. P. Wilkerson. 1989. New production in the upwelling center at Point Conception, California: temporal and spatial scales. *Deep-Sea Res.* **36**:985–1007.

Dundas, I., O. M. Johannessen, G. Berge, and B. Heimdal. 1989. Toxic algal bloom in Scandinavian waters, May–June 1988. *Oceanography.* **2**:9–14.

Foo, E.-C. 1981. A two-dimensional diabatic isopycnal model — simulating the coastal upwelling front. *J. Phys. Oceanogr.* **11**:604–626.

Franks, P. J. S. and D. M. Anderson. 1992. Alongshore transport of a toxic phytoplankton bloom in a buoyancy current: *Alexandrium tamarense* in the Gulf of Maine. *Mar. Biol.*, **112**:153–164.

Garrett, C., J. Keeley, and D. Greenberg. 1978. Tidal mixing versus thermal stratification in the Bay of Fundy and Gulf of Maine. *Atm-Oc.* **16**:403–423.

Garrett, C. J. R. and J. W. Loder. 1981. Dynamical aspects of shallow sea fronts. *Philos. Trans. R. Soc. London.* **A302**:563–581.

Garvine, R. W. and J. D. Monk. 1974. Frontal structure of a river plume. *J. Geophys. Res.* **79**:2251–2259.

Halpern, D. 1976. Structure of a coastal upwelling event observed off Oregon during July 1973. *Deep-Sea Res.* **23**:495–508.

Harris, G. P. 1980. The relationship between chlorophyll *a* fluorescence, diffuse attenuation changes and photosynthesis in natural phytoplankton populations. *J. Plankton Res.* **2**:109–127.

Holligan, P. M. 1981. Biological implications of fronts on the northwest European continental shelf. *Philos. Trans. R. Soc. London.* **A302**:547–562.

Holligan, P. M., P. LeB. Williams, D. Purdee, and R. Harris. 1984. Photosynthesis, respiration and nitrogen supply of plankton populations in stratified, frontal and tidally mixed shelf waters. *Mar. Ecol. Prog. Ser.* **17**:201–213.

Holligan, P. M., M. Viollier, C. Dupouy, and J. Aikens. 1983. Satellite studies on the distributions of chlorophyll and dinoflagellate blooms in the western English Channel. *Cont. Shelf Res.* **2**:81–96.

Houghton, R. W. and J. Marra. 1983. Physical/biological structure and exchange across the thermohaline shelf/slope front in the New York Bight. *J. Geophys. Res.* **88**:4467–4481.

Hsueh, Y. and B. Cushman-Roisin. 1983. On the formation of surface to bottom fronts over steep topography. *J. Geophys. Res.* **88**:743–750.

James, I. D. 1988. Experiments with a numerical model of coastal currents and tidal mixing fronts. *Cont. Shelf Res.* **8**:1275–1297.

Jones, B. H., L. P. Atkinson, D. Blasco, K. H. Brink, and S. L. Smith. 1988. The asymmetric distribution of chlorophyll associated with a coastal upwelling center. *Cont. Shelf Res.* **8**:1155–1170.

Jones, B. H. and D. Halpern. 1981. Biological and physical aspects of a coastal upwelling event observed during March–April 1974 off northwest Africa. *Deep-Sea Res.* **28A**:71–81.

Kishi, M. and S. Ikeda. 1986. Population dynamics of 'red tide' organisms in eutrophicated coastal waters — numerical experiment of phytoplankton bloom in the East Seto Inland Sea. *Jpn. Ecol. Modelling.* **31**:145–174.

Legendre, L., S. Demers, and D. LeFaivre. 1986. Biological production at marine ergoclines. **In:** *Marine Interfaces Ecohydrodynamics,* pp. 1–30. (J. C. Nihoul, Ed.) Amsterdam: Elsevier.

Lewis, M. R., E. P. W. Horne, J. J. Cullen, N. S. Oakey, and T. Platt. 1984. Turbulent motions may control phytoplankton photosynthesis in the upper ocean. *Nature.* **311**:49–50.

Loder, J. W. and D. A. Greenberg. 1986. Predicted positions of tidal fronts in the Gulf of Maine region. *Cont. Shelf Res.* **6**:397–414.

Loder, J. and T. Platt. 1985. Physical controls on phytoplankton production at tidal fronts. **In:** *Proceedings of the 19th European Marine Biology Symposium,* pp. 3–22. (P. E. Gibbs, Ed.) Cambridge: Cambridge University Press.

Marra, J. 1978. Phytoplankton photosynthetic response to vertical movement in a mixed layer. *Mar. Biol.* **46**:203–208.

Marra, J., R. W. Houghton, D. C. Broadman, and P. T. Neale. 1982. Distributions of chlorophyll *a* and temperature at a shelf-break front. *J. Mar. Res.* **40**:575–591.

Margalef, R. 1978. Life forms of phytoplankton as survival alternatives in an unstable environment. *Oceanol. Acta.* **1**:493–509.

Mooers, C. N. K., C. A. Collins, and R. L. Smith. 1976. The dynamic structure of the frontal zone in the coastal upwelling region off Oregon. *J. Phys. Oceanogr.* **6**:3–21.

Mooers, C. N. K., C. N. Flagg, and W. C. Boicourt. 1978. Prograde and retrograde fronts. **In:** *Oceanic Fronts in Coastal Processes,* pp. 43–58. (M. Bowman and W. Esaias, Eds.) New York: Springer-Verlag.

Mork, M. 1981. Circulation phenomena and frontal dynamics of the Norwegian coastal current. *Philos. Trans. R. Soc. London.* **A302**:635–647.

Okubo, A. 1971. Oceanic diffusion diagrams. *Deep-Sea Res.* **18**:789–802.

Ou, H. W. 1984. Wind-driven motion near a shelf-slope front. *J. Phys. Oceanogr.* **14**:985–993.

Pingree, R., M. J. Bowman, and W. E. Esaias. 1978. Headland fronts. **In:** *Oceanic Fronts in Coastal Processes,* pp. 78–86. (M. Bowman and W. Esaias, Eds.) New York: Springer-Verlag.

Pingree, R. D., G. Forster, and G. Morrison. 1974. Turbulent convergent tidal fronts. *J. Mar. Biol. Assoc. U.K.* **54**:469–479.

Pingree, R. D. and D. K. Griffiths. 1978. Tidal fronts around the British Isles. *J. Geophys. Res.* **83**:4615–4621.

Pingree, R. D., P. M. Holligan, and G. T. Mardell. 1978. The effects of vertical stability on phytoplankton distributions in the summer on the northeast European shelf. *Deep-Sea Res.* **25**:1011–1028.

Pingree, R. D. and L. Maddock. 1979. Tidal flow around an island with a regularly sloping bottom topography. *J. Mar. Biol. Assoc. U.K.* **59**:699–710.

Pingree, R., P. Pugh, P. M. Holligan, and G. Forster. 1975. Summer phytoplankton blooms and red tides in the approaches to the English Channel. *Nature.* **258**:672–677.

Platt. T. 1972. Local phytoplankton abundance and turbulence. *Deep-Sea Res.* **19**:183–187.

Richardson, K. 1985. Plankton distribution and activity in the North Sea/Skaggerak-Kattegat frontal area in April 1984. *Mar. Ecol. Prog. Ser.* **26**:233–244.

Richardson, K., M. F. Lavin-Peregrina, E. G. Mitchelson, and J. H. Simpson. 1985. Seasonal distribution of chlorophyll a in relation to physical structure in the western Irish Sea. *Oceanol. Acta.* **8**:77–86.

Rojas de Mendiola, B. 1979. Red tide along the Peruvian coast. **In:** *Toxic Dinoflagellate Blooms,* pp. 183–190. (D. L. Taylor and H. H. Seliger, Eds.) Amsterdam: Elsevier.

Rojas de Mendiola, B. 1981. Seasonal phytoplankton distribution along the Peruvian coast. **In:** *Coastal Upwelling,* pp. 348–356. (F. A. Richards, Ed.) Washington, D.C.: American Geophysical Union.

Savidge, G. 1976. A preliminary study of the distribution of chlorophyll a in the vicinity of fronts in the Celtic and Western Irish Seas. *Estuarine Coastal Mar. Sci.* **4**:617–625.

Shannon, L. V. 1985. The Benguela ecosystem. I. Evolution of the Benguela, physical features and processes. **In:** *Oceanography and Marine Biology. An Annual Review 23,* pp. 105–182. (M. Barnes, Ed.) Aberdeen: University Press.

Simpson, J. H., C. Allen, and N. Morris. 1978. Fronts on the continental shelf. *J. Geophys. Res.* **83**:4607–4614.

Simpson, J. H., D. J. Edlestein, A. Edwards, N. C. G. Morris, and P. B. Tett. 1979. The Islay Front: physical structure and phytoplankton distribution. *Estuarine Coastal Mar. Sci.* **9**:713–726.

Simpson, J. H. and J. R. Hunter. 1974. Fronts in the Irish Sea. *Nature.* **250**:404.

Simpson, J. H. and P. B. Tett. 1986. Island stirring effects on phytoplankton growth. **In:** *Lecture Notes on Coastal and Estuarine Studies 17: Tidal Mixing and Plankton Dynamics*, pp. 41–76. (M. J. Bowman, C. M. Yentsch, and W. T. Peterson, Eds.) Berlin: Springer-Verlag.

Simpson, J. H., P. B. Tett, M. L. Argotte-Espinoza, A. Edwards, K. J. Jones, and G. Savidge. 1982. Mixing and phytoplankton growth around an island in a stratified sea. *Cont. Shelf Res.* **1**:15–31.

Small, L. F. and D. W. Menzies. 1981. Patterns of primary productivity and biomass in a coastal upwelling zone. *Deep-Sea Res.* **28A**:123–149.

Smith, W. O., G. W. Heburn, R. T. Barber, and J. J. O'Brien. 1983. Regulation of phytoplankton communities by physical processes in upwelling systems. *J. Mar. Res.* **41**:539–556.

Sverdrup, H. U. 1953. On conditions for the vernal blooming of phytoplankton. *J. Cons. Int. Explor. Mer.* **18**:287–295.

Tang, C. L. 1983. Cross-front mixing and frontal upwelling in a controlled quasi-permanent density front in the Gulf of St. Lawrence. *J. Phys. Oceanogr.* **13**:1468–1481.

Tett, P. 1981. Modelling phytoplankton production at shelf-sea fronts. *Philos. Trans. R. Soc. London.* **A302**:605.

The Coastal Transition Zone Group. 1988. The coastal transition zone program. *Eos.* **69**:698–699, 704, 707.

Townsend, D. W., C. M. Yentsch, C. E. Parker, W. M. Balch, and E. D. True. 1983. An island mixing effect in the coastal Gulf of Maine. *Helgoländer Meeresunters.* **36**:347–356.

Traganza, E. D., D. G. Redalje, and R. W. Garwood. 1987. Chemical flux, mixed layer entrainment and phytoplankton blooms at upwelling fronts in the California coastal zone. *Cont. Shelf Res.* **7**:89–105.

van Heijst, G. J. F. 1986. On the dynamics of a tidal mixing front. **In:** *Marine Interfaces Ecohydrodynamics*, pp. 165–194. (J. C. Nihoul, Ed.) Amsterdam: Elsevier.

Videau, C. 1987. Primary production and physiological state of phytoplankton at the Ushant tidal front (west coast of Brittany, France). *Mar. Ecol. Prog. Ser.* **35**:141–151.

Vincent, W. F., F. H. Chang, A. Cole, M. T. Downes, M. R. James, L. May, M. Moore, and P. H. Woods. 1989. Short-term changes in planktonic community structure and nitrogen transfers in a coastal upwelling system. *Estuarine Coastal Shelf. Sci.* **29**:131–150.

Walsh, J. E., T. E. Whitledge, J. C. Kelley, S. A. Huntsman, and R. D. Pillsbury. 1977. Further transition states of the Baja California upwelling ecosystem. *Limnol. Oceanogr.* **22**:264–280.

White, A. W. 1976. Growth inhibition caused by turbulence in the toxic marine dinoflagellate *Gonyaulax excavata*. *J. Fish. Res. Board Can.* **33**:2598–2602.

Wilkerson, F. P. and R. C. Dugdale. 1987. The use of large shipboard barrels and drifters to study the effects of coastal upwelling on phytoplankton nutrient dynamics. *Limnol. Oceanogr.* **32**:368–382.

Winant, C. D. 1980. Downwelling over the Southern California shelf. *J. Phys. Oceanogr.* **10**:791–799.

Wolanski, E., J. Imberger, and M. L. Heron. 1984. Island wakes in shallow coastal waters. *J. Geophys. Res.* **89**:10553–10569.

Yentsch, C. S. 1974. The influence of geostrophy on primary production. *Tethys.* **6**:111–117.

Yentsch, C. S. and N. Garfield. 1981. Principal areas of vertical mixing in the waters of the Gulf of Maine, with references to the total productivity of the area. **In:** *Oceanography from Space*, pp. 303–312. (J. F. N. Gower, Ed.) New York: Plenum Press.